Acta Geotechnica
https://doi.org/10.1007/s11440-023-01915-3

RESEARCH PAPER

Effect of drainage conditions on CPT resistance of silty sand: physical model and field tests

Nurhan Ecemis[1] · Mustafa Sezer Arik[1] · Hazal Taneri[1]

Received: 18 May 2022 / Accepted: 24 March 2023

Abstract
The influence of drainage conditions on cone penetration test (CPT) resistance and the excess pore pressure during cone penetration in sand and silty sand are examined using field and physical model tests. Drainage can generally occur in saturated clean sand and silty sand under certain conditions. This work aims to understand and explain the effect of sand and silty sand drainage conditions on CPT resistance and pore pressure through the coefficient of consolidation (c_h) and penetration rate (v). The physical model test results indicate the significant effect of excess pore pressures and their dissipation rates, depending on the coefficient of consolidation (silt content) and the penetration rate on cone resistance. For the same relative density, normalized CPT resistance decreases as there is a reduction in c_h (or an increase in silt content) or an increase in penetration rate. The difference in CPT resistance in silty sand is attributed to drainage conditions. Finally, the results revealed in this study and the field test data reported in the literature were combined to develop an equation for the effect of drainage conditions on excess pore water pressure and CPT resistance.

Keywords Cone penetration resistance · Normalized penetration rate · Partial drainage · Silty sands

1 Introduction

In practice, many engineers use a repeatable and reliable cone penetration test (CPT) in the field. However, despite its widespread application, the influence of partially drained and undrained penetration on excess pore water pressure (u) and cone resistance (q_c) is poorly known. It may be argued that if the stress–strain characteristics and fines content of the two soils are the same, the q_c would be identical in both soils if the penetration rate is fast enough for partial drainage around the probe to be negligible or slow enough for fully drained conditions to develop around the probe. In reality however, even if the stress–strain characteristics and fines content of the two soils are the same, the degree of drainages around the probe are not the same for the same rate of penetration due to critical differences in the consolidation behavior of the soils. Therefore, the excess pore water pressure and penetration resistances would be different. Identifying the effect of permeability, k; horizontal coefficient of consolidation, c_h; and compressibility, m_v, in the sand-silt mix is important, as these parameters play a significant role in generating pore pressure during CPT penetration. Limited experimental research has been carried out to determine the effects that fines have on the k, c_h, and m_v of sand [1, 43]. In this study, the undrained, partially drained, and drained conditions of soil during CPT tests are related to the parameter T (= vd/c_h) involving c_h, and the non-soil-property-related factors, the penetration rate, v, and cone diameter, d [34]. The coefficient of consolidation can be interpreted by either laboratory-based tests or in-situ tests, such as the CPTu pore pressure dissipation test (PPDT). Moreover, it is also possible to characterize c_h probabilistically [47].

This work aims to examine the effect of sand and silty sand drainage conditions on pore pressure and cone resistance through the c_h and v, at different relative densities (D_r). A group of twelve sets of tests—piezocone penetration (CPTu), direct push permeability (DPPT), and seismic piezocone penetration (SCPTu)—was performed side by side in a soil box with fully saturated clean sand and silty

✉ Nurhan Ecemis
nurhanecemis@iyte.edu.tr

[1] Civil Engineering Department, Izmir Institute of Technology, Urla, Izmir 35430, Turkey

Published online: 18 June 2023

sand at 5%, 15%, and 35% silt content. The piezocone penetration test can not only provide CPT test results but also measure in-situ pore water pressure. The CPTu test provides continuous and simultaneous readings of q_c, sleeve friction (f_s), and u. The SCPTu is an effective testing tool to measure the shear wave velocity (V_s), which is closely related to the mechanical properties of the soil. Duan et al. [10] evaluated the undrained shear strength from the V_s values. In this study, the V_s data obtained from the SCPTu tests were used to find the compressibility of the soil. The DPPT tool is a combination of a specially fabricated cylinder with valve attachment points for water and compressed gas inlets/outlets, and a screened probe [26]. The DPPT test is used to find the k value of clean sand and silty sand.

In the first part of this study, the effect of k, c_h, and m_v in the sand-silt mix was identified by the experimental research. Then, the combined effect of the c_h and v on the penetration process changed from drained to undrained conditions, particularly in silty sands. It is worth mentioning that in this study, T is controlled by the soil's c_h and v for a constant diameter of the cone. In the second part of this study, four sets of field tests (SCPTu, pore pressure dissipation, DPPT, and standard penetration) that were conducted at silty sand sites [12] were examined to understand the drainage effects for both loose and dense soil covering higher T values. Finally, the laboratory test results were combined with data from the field tests to assess the limit T values for undrained (T_{undr}) and drained (T_{dr}) conditions.

1.1 Basic knowledge of drainage conditions on CPT resistance

Several researchers have taken into consideration the drainage condition effect in their experimental [5, 9, 18, 20, 23, 24, 30, 37] and numerical investigations [3, 14, 17, 18, 20, 40, 46] by studying the effect of the c_h, v, and d on the cone tip resistance and excess pore pressure during the cone penetration into the soil. Schneider et al. [37] found that the overconsolidation ratio and silt content significantly affected the q_c and u. Kim et al. [21] suggested the limiting values of T for drained and undrained conditions as 0.05 and 10, respectively. Ecemis [14] noted that the drained condition occurs at $T < 0.01$, and the undrained condition occurs at $T > 6$. Jaeger et al. [20] performed centrifuge experiments using 75% sand and 25% kaolin at variable penetration rates. They found the T for drained and undrained transition points between 0.01 and 20. Oliveira et al. [30] used centrifuge tests performed at variable v values using a mini-CPT probe and presented an analytical approach. Their research found the transition value of T for drained and undrained conditions between 1 and 75, respectively.

Kokusho et al. [23] examined the impact of non- or low-plastic silt and clay particles on the cone resistance by using a miniature cone in triaxial equipment. They noticed that for a given D_r, cone resistance decreased, and excess pore pressure increased as the result of an increase in fines content. In their research, the d of the cone and v were small, which may lead to partially drained or even drained conditions, even if the CPT is performed at the highest fine content of 30%. Yi et al. [46] reported that the T values for drained and undrained conditions were 0.1 and 10, respectively. DeJong and Randolph [8] found T for drained and undrained conditions between to be 0.3 and 30, while Mahmoodzadeh and Randolph [28] indicated transition T values of 0.1 and 10, respectively. In a different D_r, Huang [18] provided a qualitative understanding of how the effect of fines influences the cone resistance in silty sand. They suggested drained conditions for T at less than 0.04 and undrained conditions for T at more than 10. Ceccato and Simonini [3] found T values for drained and undrained transition points between 0.2 and 60, respectively. Chow et al. [5] investigated the change in q_c in the sand at various v values using centrifuge piezocone tests. The results indicated that the q_c increases with increasing v in dense sand but reduces with increasing v in loose sand.

2 Experimental study

2.1 Soil properties

Sand and silt that were used in the experiments were obtained from the city of Izmir and Kirklareli, respectively. Based on the Unified Soil Classification Scheme, the clean sand was defined as poorly graded sand (SP), and the sand-silt mixture was described as silty sand (SM). Figure 1a displays the clean sand and sand-silt mixture's grain size curves with silt (fine) contents (FC) of 5%, 15%, and 35%. The effective particle size (D_{10}), the mean grain size (D_{50}), the coefficient of uniformity (C_u), the specific gravity (G_s), Poisson's ratio (v), and the maximum void ratio (e_{max}) and minimum void ratio (e_{min}) values of the sand-silt mixtures are listed in Table 1. Accurate v measurement is complicated in the laboratory due to the bedding errors and system obedience [27]. Therefore, Suwal and Kuwano's [41] method was used to assess the v of silty sands in saturated conditions.

Each silty sand sample's e_{max} and e_{min} values were obtained by the method of Lade et al. [25]. The fines content range investigated in this study is greater than what is allowed by many standards. Therefore, a nonstandard procedure [25] was chosen in this study, which had been

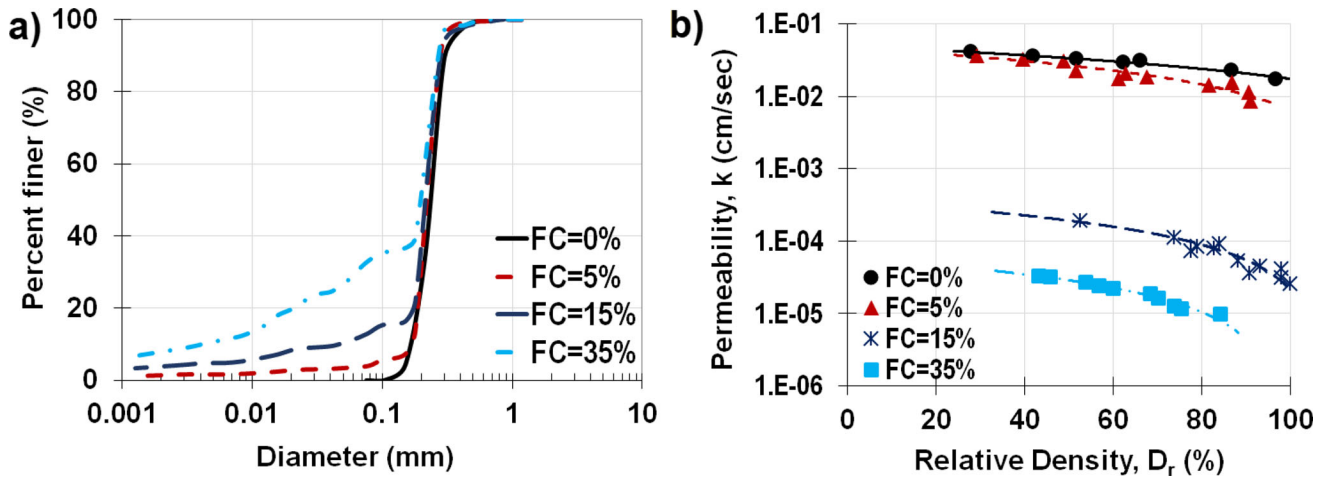

Fig. 1 **a** Gradation curves, and **b** variation of permeability with D_r at clean sand and sand-silt mix of 5%, 15%, and 35% fines content

Table 1 Physical properties of sand and silty sand

Parameters	Silt content (%)			
	0	5	15	35
G_s	2.64	2.64	2.65	2.66
D_{10}	0.17	0.17	0.05	0.005
D_{50}	0.24	0.22	0.22	0.20
C_u	1.50	1.37	4.52	46.67
C_C	1.03	1.07	3.26	4.20
e_{max}	1.00	0.94	0.88	0.83
e_{min}	0.72	0.68	0.58	0.43
ν	0.25	0.30	0.35	0.40

successfully used for obtaining the e_{max} and e_{min} of various silty sands in the literature [45]. The e_{max} and e_{min} values decrease as the fines content increases.

The constant head tests were performed to find the k values of clean sand and silty sand with 5% FC, and falling head permeability tests were performed for soils with 15% and 35% FCs. The results show that the *k* values of clean and silty sand are not the same, even at the same D_r. The k of saturated sand containing 5% silt is roughly less than a half order of magnitude smaller than the k of clean sand; however, both curves (0% and 5% FC) come close to each other as soils become loose. The permeability of saturated sand containing 15% silt is almost two orders of magnitude smaller than the k of clean sand. The significant drop in the *k* value with an increase of FC toward 15% is mainly due to the reduced pore size within the grain matrix. The measured k values of clean sand and 5% silt are influenced relatively less by the change in D_r within the studied range, although less than half an order of decrease in k is observed with an increasing D_r. However, the sensitivity of *k* to D_r is more noticeable at FC = 15% and 35%. Hence, for FC = 15% or 35%, the k could range within one order of magnitude, depending on the D_r. The relationship between k and D_r for the soils used in the tests is presented in Fig. 1b.

2.2 Laboratory testing procedure

For each saturated clean sand and sand-silt mix at different silt contents (5%, 15%, and 35%), a total of three tests—(a) CPTu, (b) SCPTu, and (c) DPPT—were conducted inside the rectangular box with a spacing of 40 cm to examine the effect of c_h (or fines), v, and D_r on the excess pore pressure and the cone resistance. Figure 2 displays the side view of these test positions. This close spacing

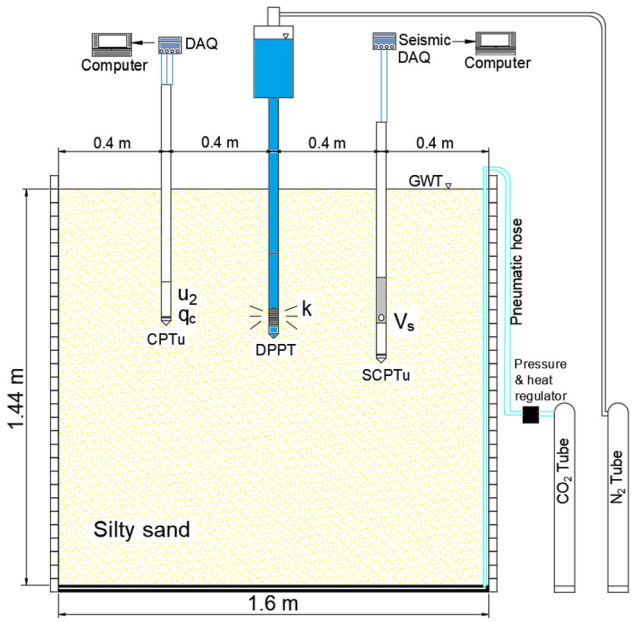

Fig. 2 Schematic view of CO_2 and N_2 gas injection system, and side view of CPTu, SCPTu, DPPT tests conducted inside the box

between the tests had the potential to influence the test results, were there to be any interference from previous soundings. For instance, the DPPT test could have affected the cone penetration test results as water is injected to the soil. To eliminate the possibility of the test results affecting one another, it was decided that the sequence of the tests conducted inside the box would be CPTu, SCPTu, and DPPT.

2.2.1 Soil box sample preparation

The samples were deposited inside a rigid, rectangular large-scale box that had internal dimensions of 45 cm width, 163 cm length, and 150 cm height. Three clean sands (S1 to S3) and nine sand-silt mixtures (S4 to S12), each of which was 144 cm in height, were prepared inside the box by the dry pluviation method. With this method, dry soil is deposited directly inside the box from 10 cm above the ground surface to diminish silty sand's particle segregation [45]. At each fines content (0%, 5%, 15%, and 35%), soil samples were prepared at three different densities (loose, medium dense, and dense).

The sample preparation procedure involved several steps. First, dry sand and silt were intermixed. Then, the membrane was placed inside the box. A 3-mm diameter pneumatic hose was put on the membrane to apply carbon dioxide (CO_2) gas, which has a high water solubility from the bottom of the soil sample. A funnel was used to slowly pour the dry soil into a box up to a depth of 144 cm. During the filling process, the soil was tamped to obtain medium-dense and dense soils. Throughout the depth, the tamping was performed at ten different layers. The soil was tamped from the surface of each layer two and five times to have medium dense and dense soils, respectively. For each specimen, the average D_r is assessed by recording the weight of each prepared dry sample and water supplemented to the model. It was difficult to obtain constant D_r within the large box throughout the depth. Hence, during the preparation of the samples, the D_r changed slightly throughout the depth. As it is crucial to find the D_r at specific depths inside the box, the D_r values at specific depths were determined using a different method, which is explained in the following sections.

The silty sand must be fully saturated. Therefore, CO_2 was introduced into the soil for almost 60 min from the bottom of the soil box to remove the bubbles throughout the soil. The water was permitted to run from the bottom of the soil after the percolation of CO_2 into the box. The entire volume of water introduced into the sample was recorded through the sample preparation. A layer of water with a constant height of 5 cm was maintained above the soil surface. The schematic view of the homogeneous silty sand specimen, CO_2 tube, and the pressure and heat regulators are illustrated in Fig. 2.

2.2.2 Piezocone penetration test (CPTu)

A total of twelve CPTu tests were carried out in the box using clean sand and three different sand-silt mixes at FC of 5%, 15%, and 35% by dry weight. Using a reaction frame and hydraulic pushing system, the CPTu tests were performed at cone penetration velocities from 0.8 to 1.5 cm/sec. The complete CPTu testing system used in the laboratory was comprised of a cone probe, CPTu rods, a depth encoder, and a data acquisition system (DAQ). The probe used in the CPTu tests had a shaft diameter of 35.7 mm and a 60° tip angle. The penetration depth, cone penetration resistance, and pore water pressure above the cone shoulder (u_2) for each 1 cm of penetration were digitized inside the probe and transferred to the DAQ. Before starting each piezocone test, glycerin was used to thoroughly saturate the porous stone [36].

The percentage of the box diameter to the CPT probe ($R_d = D_c/d_c$) is the main factor that affects the cone penetration and pore pressure measurements inside the box. In this study, cone penetrations were performed along one concentric circle, with the outer circle being 45 cm from the box boundary. Using 45 cm as the distance to the side gives an R_d value of 13 for the cone with a diameter of 3.57 cm. Several researchers [16, 32, 33, 35] have studied the effects of boundary conditions on CPTu data and whether the boundary conditions of the calibration chamber can model the in-situ free field conditions. For a rectangular box, Gui et al. [16] reported that there was not much deviation in normalized cone penetration resistance (q_{c1N}), as the R_d value exceeded 11. Hence, the limit conditions of the box can reasonably simulate the free-field conditions. More details of the effect of boundary conditions of the box on CPTu measurements can be found in Ecemis [11].

The measured q_c values, shown in Fig. 3a-d, need to be normalized to reflect the soil type and stiffness of granular soils. In this study, CPTu measurements were obtained at shallow depths and low effective stress levels of less than 1 atm. Therefore, the normalization equation and stress normalization exponent, c, that was proposed by Olsen [31] was used to normalize the recorded penetration resistance:

$$q_{c1N} = \frac{q_c - \sigma_{vo}}{\left(\sigma'_{vo}\right)^c} \quad (1)$$

$$c = 1 - (D_r - 10\%) \times 0.007 \quad (2)$$

where σ_{vo} is the total vertical stress, σ_{vo}' is the effective vertical stress, and q_c is the cone tip resistance in units of

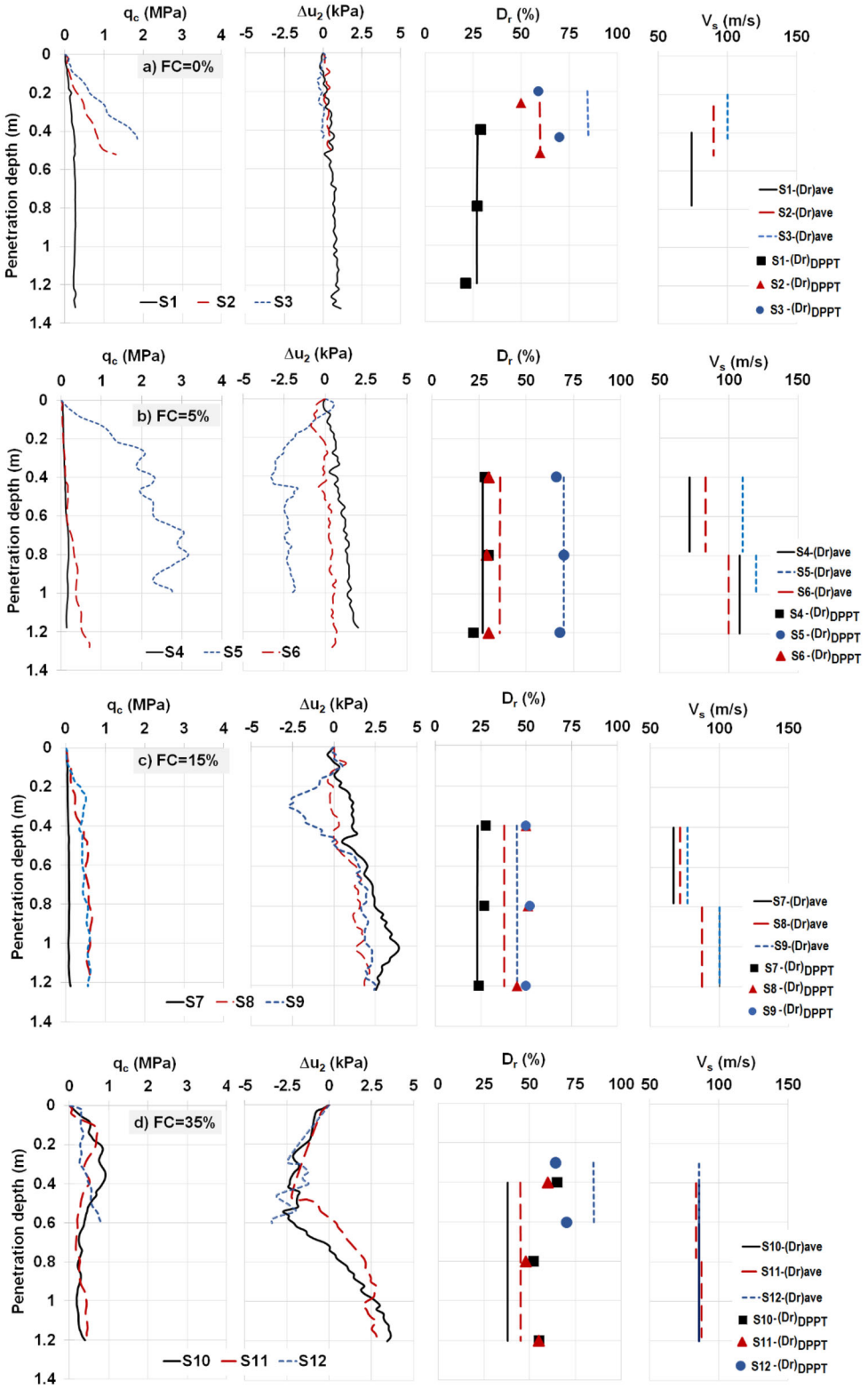

Fig. 3 Cone tip resistance, excess pore water pressure, relative density, and shear wave velocity of **a** clean sand, **b** FC = 5%, **c** FC = 15%, and **d** FC = 35%

atm. In this study, for a D_r of 70% to 21%, the value of c ranged from 0.58 to 0.92, respectively.

2.2.3 Seismic CPTu test

After the CPTu tests, based on the ASTM D5778-12 standard, SCPTu tests were done. The SCPTu tests were performed 0.8 m away from the CPTu borehole (Fig. 2). During the SCPTu tests, q_c, f_s, and u_2 for each 1 cm of penetration can be measured. However, the particular time gap to measure V_s had the potential to influence the measured CPT resistance and pore water pressure values. Therefore, only V_s data were taken from the SCPTu tests. As illustrated in Fig. 4, the seismic cone that was attached to the classic CPTu probe was pushed into the soil. The S-plate, which was placed 1 m away from the borehole, was laterally stroked with a hammer, and the S-waves transmitted to the seismometer inside the CPTu probe.

The shear wave velocities were calculated with the cross-correlation method at subsequent depths. The cross-correlation method uses all shear wave signals to measure the time at which the low signal is shifted to the high signal. After shifting entire signals, the sum of the products of these signals' amplitudes and the most significant time shift in the signal time graph was used to calculate the V_s [2]. Filtering was used in the cross-correlation method to avoid unwanted noises in the signals and obtain pure shear waves. Figure 3a-d shows the V_s values measured at several depths for each prepared sample (S1–S12).

2.2.4 Direct push permeability test

Following the SCPTu test, the k values were obtained by DPPT at the depths where the SCPTu tests were done. Figure 2 schematically shows the DPPT testing location. DPPT testing equipment used in the experiments has the following parts: a specially fabricated cylinder tank with water and compressed nitrogen gas inlets and outlets, a 60° tapered tip and a 3.57 cm diameter probe [26], and a perforated screen with a length of 45 mm and slit size of 0.3 mm (Fig. 5).

During the DPPT, the cylinder tank was filled with water, and then water was pressurized from the top by nitrogen. The water flow rate from the screen was then recorded manually as water discharge of water to the soil. The hydraulic conductivity of each sample is determined as [26]:

$$k_h = \frac{Q}{4\pi \Delta h a_s} \tag{3}$$

where Q is the measured volumetric flow, Δh is the excess head, and a_s is the radius of the perforated screen. In this

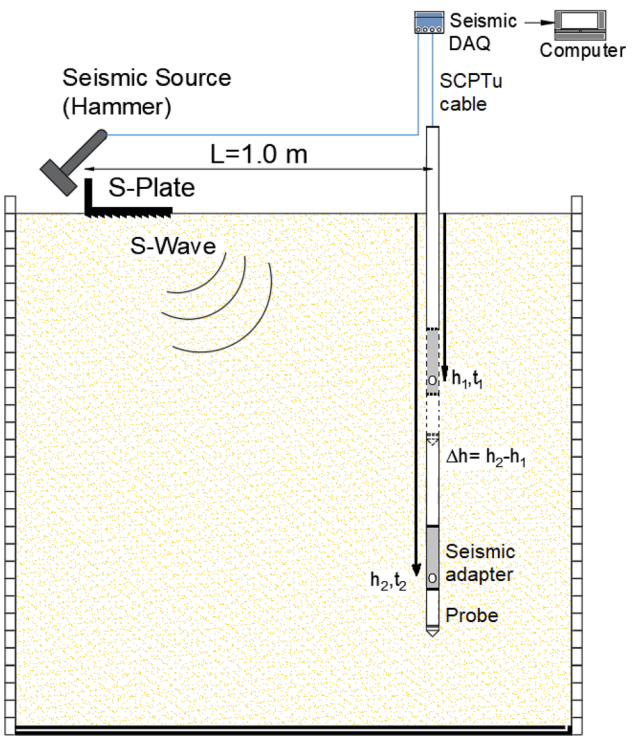

Fig. 4 Schematic view of SCPTu performed in the laboratory

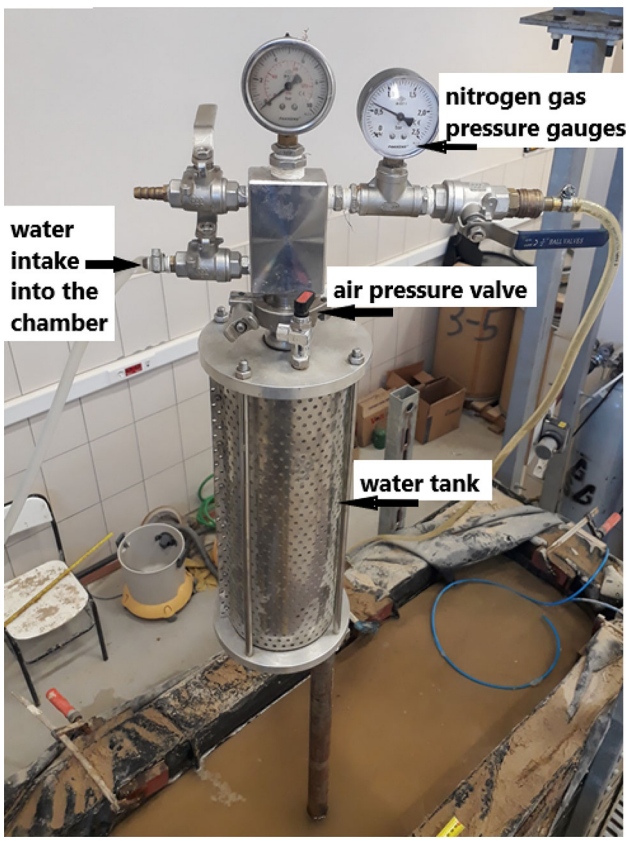

Fig. 5 DPPT test performed in the laboratory

study, a_s is 1.44 cm. Additionally, using the relationship between k and D_r (Fig. 1b) for each soil, and the measured k values at desired depths inside the box, one can obtain the relative density of the prepared soil sample at specific depths. As the relative density was obtained from the DPPT tests, it is labeled as $(D_r)_{DPPT}$. The average relative density, $(D_r)_{ave}$, was obtained by recording each prepared sample's dry weight and the quantity of water supplemented to the specimen. Figure 3a-d shows the $(D_r)_{ave}$ and $(D_r)_{DPPT}$ in each sample at particular depths. To exemplify, the $(D_r)_{DPPT}$ of the S1-specimen was found at 21% to 29% through the depth. For this specimen, the $(D_r)_{ave}$ obtained was 27%. These comparisons revealed that the $(D_r)_{DPPT}$ assessed from the relationship between k and D_r agrees with the $(D_r)_{ave}$ obtained by recording the weight of each prepared dry sample and the water supplemented to the soil. In this study, the relative density values that are obtained by using the DPPT tests are used in further analyses.

3 Experimental results and discussion

3.1 Permeability and coefficient of consolidation in sand-silt mix

It is important to know the effect of k, c_h, and m_v in the sand-silt mix to identify the impact of drainage conditions in generating pore water pressure and cone penetration resistance during CPT tests. Figure 1b and $(D_r)_{DPPT}$ obtained at significant depths inside the box were used together to determine the k of the prepared sand-silt mixtures. The permeability values of clean sand and silty sand are different at the same D_r. Adding 5% silt to the sand decreased its k value a half order of magnitude compared to the clean sand (FC = 0%) at a given D_r. However, k decreases rapidly as FC in sand increases to 15% and 35%. The permeability of saturated soil with FC = 15% is almost two orders of magnitude smaller than the k of soil with FC = 0%. The permeability ranges mostly within one order of magnitude from FC 15% to 35% at a given D_r. The reduced pore size is the main reason for the substantial drop in k values with an increase in FC up to 35%. Figure 6a shows the variation of k with various D_r values at different FCs. The sand-silt mixture's c_h within the box was calculated as:

$$c_h = \frac{k}{m_v \gamma_w} \tag{4}$$

where γ_w is the unit weight of water, and m_v was derived from the SCPTu test data as:

$$m_v = \frac{1.5(1-2v)}{V_s^2 \rho (1+v)} \tag{5}$$

where ρ is the density, and v is the Poisson's ratio of the soil samples. It is found that m_v mostly depends on the soil fabric and the pore size, not on the FC of the soil. It can be clearly seen from Fig. 6b that the m_v of a different FC falls into a narrow band, and all calculated m_v values are almost in the same order of magnitude. Bandini and Sathiskumar [1] and Thevanayagam and Ecemis [43] likewise reported that changes in silt content up to about 25% silt have a minor effect on m_v values.

The c_h of FC = 5% is similar to the clean sand. However, the c_h of silty sand with FC = 15% and 35% is much smaller than the FC = 0% and 5%, even at the same D_r. The c_h reduces by about two orders of magnitude, while the FC increases to 35% compared to the c_h of clean sand. Figure 6c indicates that the change in c_h is directly related to the change in k as the reduction in k by about two orders of magnitude also decreases the c_h by about two orders of magnitude, with an increase in FC up to about 35%. The difference of c_h between clean sand and silty sand is the main reason for the difference of induced excess pore pressure dissipation time. This causes a different drainage condition, which plays an essential role in the cone resistance. At the same density, the increase of FC significantly affects the pore size and permeability, leading to a reduction in c_h. These findings also align with Thevanayagam and Ecemis's [43] studies.

3.2 Effect of D_r on excess pore pressure and cone resistance of clean sand and silty sand

For the samples with the same FC, the q_{c1N} and Δu_2 values were discussed by considering the change in D_r. At each sample, the initial penetration is characterized by a parabolic increase of the q_{c1N} with depth. After a critical depth ($z_{critical}$), the increase in q_{c1N} slows down very quickly, and the q_{c1N} implies that the soil at the tip of the cone reaches a steady state condition. The $z_{critical}$ depends on the diameter of the cone, σ_{vo}', and D_r of the soil [38]. In this study, for loose, medium dense, and dense soil deposits, the $z_{critical}$ is reached up to roughly 0.04 m, 0.1 m, and 0.25 m depths, respectively. The q_{c1N} and u values that were determined at depths greater than the $z_{critical}$ are used in the correlations.

For the clean sand (S1, S2, S3), the Δu_2 values are not significantly different, even though there is a change in $(D_r)_{DPPT}$. However, q_{c1N} changes with a change in $(D_r)_{DPPT}$. For the dense sample (S3), the u is found negative up to a depth of 0.4 m, where data are recorded. The measured negative Δu_2 from dense soil indicates soil dilation during the cone penetration. For the soils having FC values of 5% (S4, S5, S6), the q_{c1N} values at the S5 sample are considerably more significant than the samples S4 and S6. For the

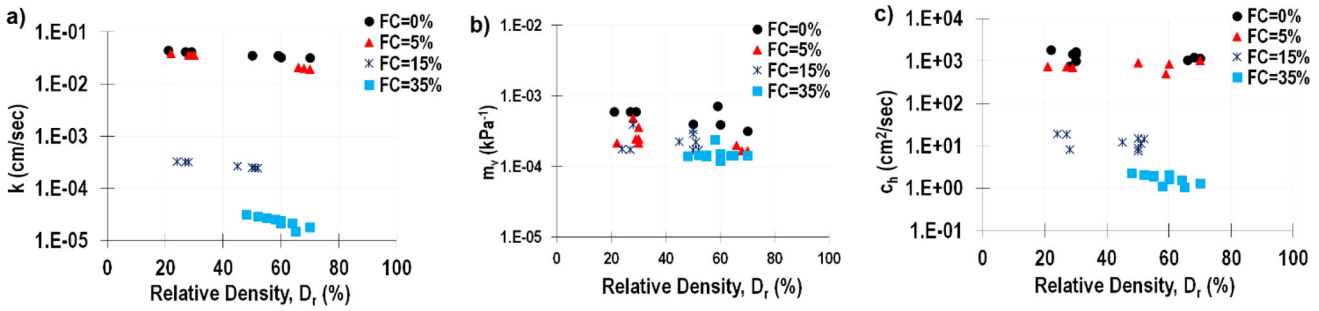

Fig. 6 Variation of **a** hydraulic conductivity, **b** compressibility, and **c** coefficient of consolidation with D_r at different FC

dense sample (S5), the u_2 is also found to be negative throughout the depth. For the soils having FC values of 15% (S7, S8, S9), the q_{c1N} values do not change significantly, even though the $(D_r)_{DPPT}$ changes from 25 to 50%. Moreover, below 0.4 m depth, the $(D_r)_{DPPT}$ at each sample is not dense (less than 50%), and the u_2 values are positive. For the soils having FC of 35% (S10, S11, S12), the soil above 0.6 m depth is dense, and the u_2 values are negative. For samples S10 and S11, below 0.6 m depth, positive u_2 is observed. Hence, the soil shows loose and medium-dense behavior.

The experimental test results were plotted to understand the effect of FC and D_r on the excess pore pressure (Fig. 7a) and the normalized penetration resistance (Fig. 7b). These figures illustrate the data corresponding to clean sand and three different FCs from 5 to 35%. The influence of FC and D_r seems to have a significant and complex effect on the u/σ_{vo}'. Still, based on Fig. 7a, one can make general observations. At each FC, the u/σ_{vo}' reduces by an increase in D_r. Adding 5% silt to the sand increased its u/σ_{vo}' compared to the clean sand at a relative density of less than 35%; however, the u/σ_{vo}' decreased as the soil became denser. Further addition of fines from 5 to 15% had systematically increased the u/σ_{vo}' at a given D_r (trend lines shifted upward). One can also observe that the clean sand curve is crossed by the 5% silty sand curve around D_r of 35%. From an FC of 15% to 35%, an increase in $\Delta u/\sigma_{vo}$' is observed for D_r less than 60%; on the other hand, the $\Delta u/\sigma_{vo}$' is smaller at $D_r > 60\%$.

As shown in Fig. 7b, the cone resistance increased with an increase in D_r for each FC, where trend lines represented the general growth. The CPT resistance decreases as FC reduces from 0 to 35% at a given D_r. A change in D_r of clean sand from 20 to 40% (loose soil) and 40% to 60% (medium dense soil) increased the q_{c1N} by a magnitude of 2.1. For FC = 5% and 15%, the increase in q_{c1N} is almost identical to the clean sand's trend. For FC = 35%, a change in D_r from 50 to 70% (medium dense to dense soil) increased the q_{c1N} by a magnitude of about 1.8, which is less than a lower FCs.

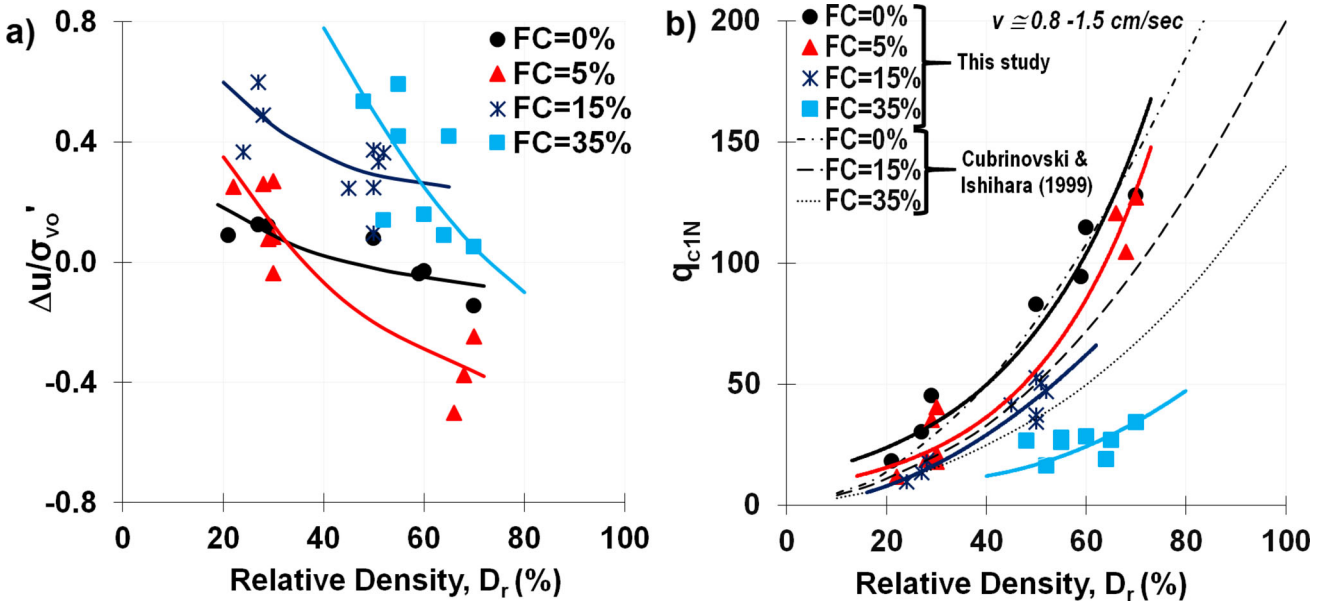

Fig. 7 Experimental test results **a** u/σ_{vo}' versus D_r, and **b** q_{c1N} versus D_r at clean sand and sand-silt mix of 5%, 15%, and 35%

The above-determined trends between q_{c1N} and D_r of clean sand (FC = 0%) compared with the study of Ghali et al. [15], and a highly similar trend is observed. Moreover, the relationships between q_{c1N} and D_r of clean sand and silty sand having 15% and 35% silts, presented in this paper, were compared by the data of Cubrinovski and Ishihara [6] (Fig. 7b). For FC = 0% and 15%, the q_{c1N} and D_r relationship obtained in this study show similar curves as the data observed in the study of Cubrinovski and Ishihara [6]. However, for FC = 35%, the q_{c1N} values developed by Cubrinovski and Ishihara [6] at a given D_r are larger than those presented in this paper.

3.3 The Role of the c_h on excess pore pressure and cone resistance

Irrespective to D_r, the T factor delimits the undrained, partially drained, and drained conditions during cone penetration to the soil sample. The limits of T values from drained to partially drained as well as partially drained to undrained conditions were determined from this study's laboratory tests. The test data are presented in Fig. 8a-b to show the change in $\Delta u/\sigma_{vo}$' by T and q_{c1N} by T at different D_r of the sand-silt mix. In each figure, the data were obtained for three different varieties of D_r ($10\% < D_r \leq 30\%$; $30\% < D_r < 60\%$; and $60\% \leq D_r \leq 70\%$). The T changed with the v, varying from 0.8 cm/sec to 1.5 cm/sec, and c_h varying from 10^2 to 10^3 cm^2/sec. Only the cone diameter was constant.

The effect of T has reflected in the $\Delta u/\sigma_{vo}$' by the change in the c_h and v. The change of T was examined from about 0.001 to about 5. For T more than 0.01, we examined an increase in $\Delta u/\sigma_{vo}$' at each D_r. For loose ($10\% < D_r \leq 30\%$) and medium dense ($30\% < D_r < 60\%$) soils, positive $\Delta u/\sigma_{vo}$' develops at each T value. For dense soils ($60\% \leq D_r \leq 70\%$), as T gets smaller, an extensive amount of negative $\Delta u/\sigma_{vo}$' develops. This clearly shows the dense soil's dilative behavior during the penetration of the cone into the soil. Also, the most significant increase with T occurs with D_r between 60 and 70%. Figure 8a shows the $\Delta u/\sigma_{vo}$' versus T at different D_r of the sand-silt mixture.

Correspondingly, depending on the D_r of the soil, we examined a decrease in q_{c1N} with an increase in T values. At high T values, longer pore water pressure dissipation occurs, and this cause causes smaller σ_{vo}' around the cone. With increasing T, the soil behavior evolved from drained to partially drained, then undrained. At the given relative density, the decrease of T from 0.001 to 0.01 caused the minimal change at $q_{c1N,}$ representing a drained penetration ($T_{dr} = 0.01$). The increase of T from 0.01 to about 5 represented the partially drained condition as q_{c1N} reduced considerably. The rise of T from 5 changed q_{c1N} in nominal values, expressing an undrained penetration ($T_{undr} = 5$). Figure 8b shows the change in q_{c1N} with T at different D_r of the sand-silt mixture. It can be concluded that instead of the FC of the soils, T is a more rational parameter to determine the degree of consolidation during cone penetration.

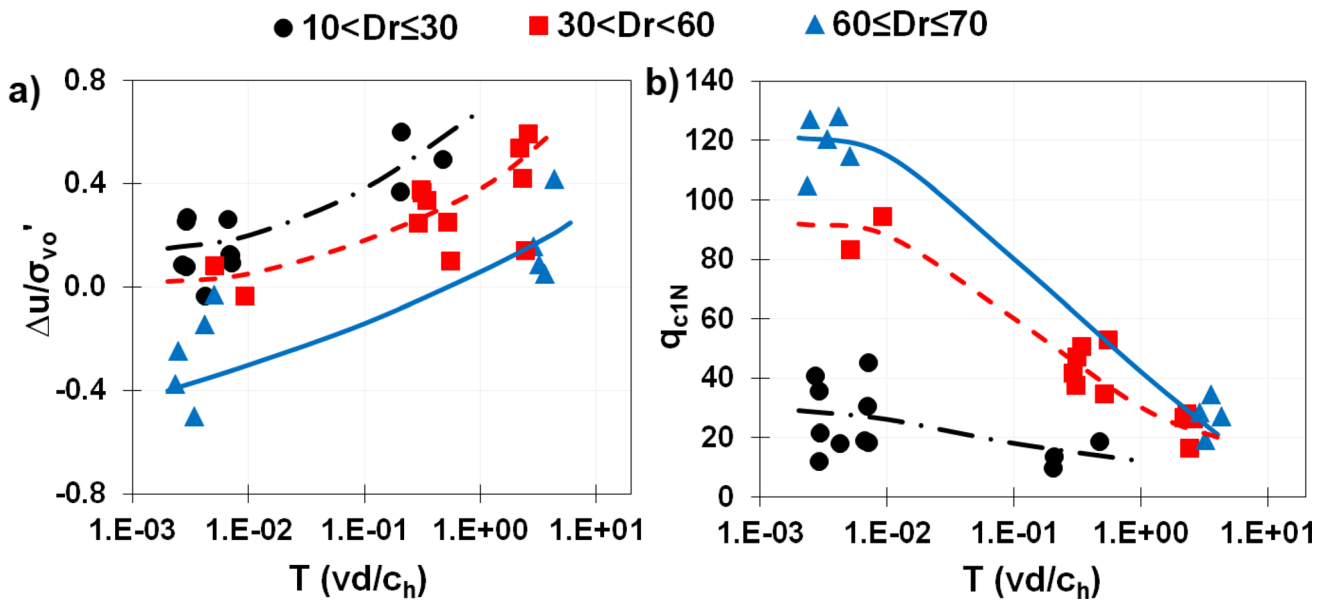

Fig. 8 Physical model test results from drained to undrained conditions: Effects of normalized penetration rate and relative density on **a** excess pore water pressure ratio, and **b** normalized cone penetration resistance

4 Field study

The effect of T and D_r on CPT resistance and the excess pore pressure response behind the cone tip, which was determined from this study, were expanded with the field test program. The field test data were reported and analyzed in the research project EU-Marie Curie IRG-248218 [13] and Ecemis and Karaman [12]. The details of the tests are explained in the mentioned studies, but some aspects were highlighted here.

The test layout, shown in Fig. 9a, applied at 20 test sites consisted of SCPTu, DPPT, pore pressure dissipation test (PPDT), and standard penetration test (SPT). As revealed in the figure, the SCPTu, PPDT, and DPPT tests were performed on the corners of the triangle grid at 2.6 m spacing. The SPT tests were performed in the middle of the grid. Illustrations of an SPT spoon sample, DPPT, PPDT, and DPPT data points with corresponding depths of SCPTu tests are presented in Fig. 9b.

A total of 174 disturbed soil samples were obtained throughout the depth from the boreholes for laboratory characterization tests (sieve analysis, hydrometer, and Atterberg limit tests). Based on the sieve analysis tests, all the samples fall in the range of coarse to fine sand and silty sand deposits. As shown in Fig. 10, a total of 25 soil samples have FC less than 5%; 81 soil samples have FC between 5 and 15%; 49 soil samples have FC between 15 and 35%; and 19 soil samples have FC from 35 to 50%. The mean grain size (D_{50}) is within the range of 0.08 mm to 0.55 mm, and the uniformity coefficient is in the range of 1.17 to 22.14. By using the Unified Soil Classification

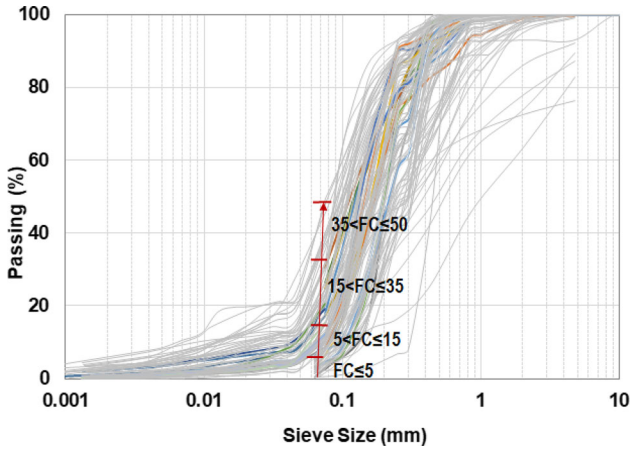

Fig. 10 Grain size distribution curves of the soils from the field investigation

System, the soil types collected from the field were classified as nonplastic, poorly graded clean sand (SP), silty sand (SM), and clayey sand (SC). Moreover, relatively small interbedded silt mixtures and clay layers were detected. Fines present in the 92 samples were nonplastic, and the rest of the samples were low plastic.

Using the equation given by Cubrinovski et al. [7], the relative density is estimated from the corrected SPT test blow counts, $(N_1)_{60}$, for 60% energy efficiency and effective overburden stress of 100 kPa:

$$D_r = \sqrt{\frac{(N_1)_{60}(0.43 + 0.0087\,FC)^{1.7}}{11.7}} \tag{6}$$

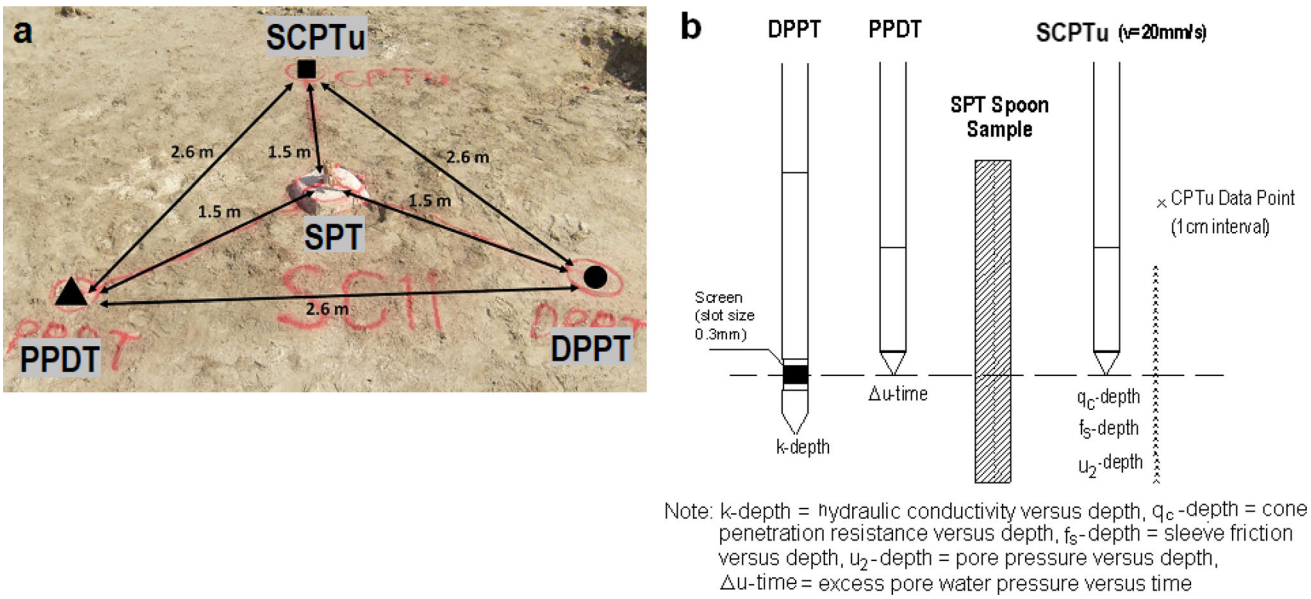

Fig. 9 **a** Typical test layout at 20 test sites, and **b** an illustration of a SPT spoon sample, DPPT, PPDT, and DPPT data points with corresponding depths of piezocone penetration test

From the field, $(N_1)_{60}$ was measured between 2 and 28, indicating the D_r value of subsoil strata between 10 (very loose) and 67 (medium dense).

4.1 Coefficient of consolidation in the field

The c_h values for each sample in the field were determined from: (1) PPDT tests, and (2) combination of DPPT (Eq. 3) and SCPTu test results (Eq. 5) that were obtained at the same depths. When the water dissipation was monotonic and nonmonotonic, the c_h was estimated using PPDT curves. However, the PPDT tests could not provide a reliable means of estimating the c_h when the drained response was observed. In those conditions, the DPPT and SCPTu tests performed in the field were used to find the c_h of these soils.

From the PPDT tests in the field, two different pore water pressure dissipation curves were obtained: Type I and Type II. These curves show the variation of Δu_2, which has been normalized by the initial pore water pressure with time. Both Type I and Type II show characteristics of undrained to partially drained silty sand soils. As shown in Fig. 11a, Type I dissipation curves show a monotonically decrease in pore water pressure, and a 50% dissipation time, t_{50}, was directly determined using monotonic reduction curves. The correlation proposed by Teh and Houlsby [42] was used to interpret the c_h values:

$$c_h = \frac{T_{50}\, r^2 \sqrt{I_r}}{t_{50}} \tag{7}$$

where r is the cone radius, I_r is the rigidity index, and T_{50} is the nondimensional time factor for a 50% pore water pressure dissipation. The rigidity index depends on the cementation effect and the anisotropic macrostructure of sediments. The influence of these factors on the value of initial shear modulus G_{max} had been demonstrated by Mlynarek et al. [29]. Hence, in this study, I_r of the soil is estimated by the equation proposed by Krage et al. [22]:

$$I_r = \left(\frac{G_{\max}}{\sigma'_{vo}}\right)\left(\frac{0.79}{\left[0.33\,\frac{q_t-\sigma_{vo}}{\sigma'_{vo}}\right]^{0.75}}\right) \tag{8}$$

The G_{max} was evaluated from the V_s and density correlation. The V_s values were determined from the SCPTu tests. Type II curves are nonmonotonic dissipation curves that show an initial increase and then a decrease in pore pressure. Sully et al. [39] proposed a solution to obtain the t_{50} for Type II curves, which show that the pore pressure distribution increases in a positive direction. They ignored the increase in pore pressure distribution part and focused instead on the reduction in pore pressure distribution. Hence, the t_{50} calculations did not consider the influence of the initial excess pore pressure. Later, Chai et al. [4] investigated t_{50} by considering the effect of the initial increment in a positive direction. They proposed an empirical formula to get the corrected value of t_{50} from the nonstandard dissipation curve. In this study, Chai et al.'s [4] method was used to determine the corrected time of t_{50} for nonstandard curvatures, as shown in Fig. 11b, which have increments in both negative and positive directions:

$$(t_{50})_c = \frac{t_{50}}{1 + 18.5\left(\frac{t_{u,\max}}{t_{50}}\right)^{0.67}\left(\frac{I_r}{200}\right)^{0.3}} \tag{9}$$

where $t_{u,max}$ is the time for maximum excess pore water pressure that was obtained between 30 and 150 s.

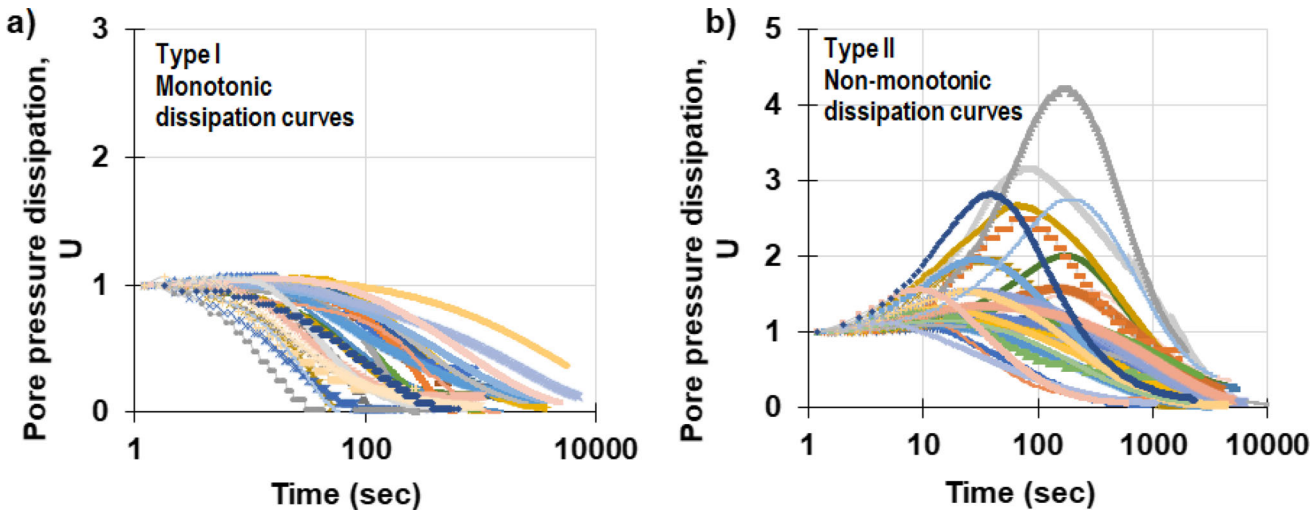

Fig. 11 Two types of pore pressure dissipation curves for undrained to partially drained dissipation; **a** Type I, and **b** Type II obtained from PPDT

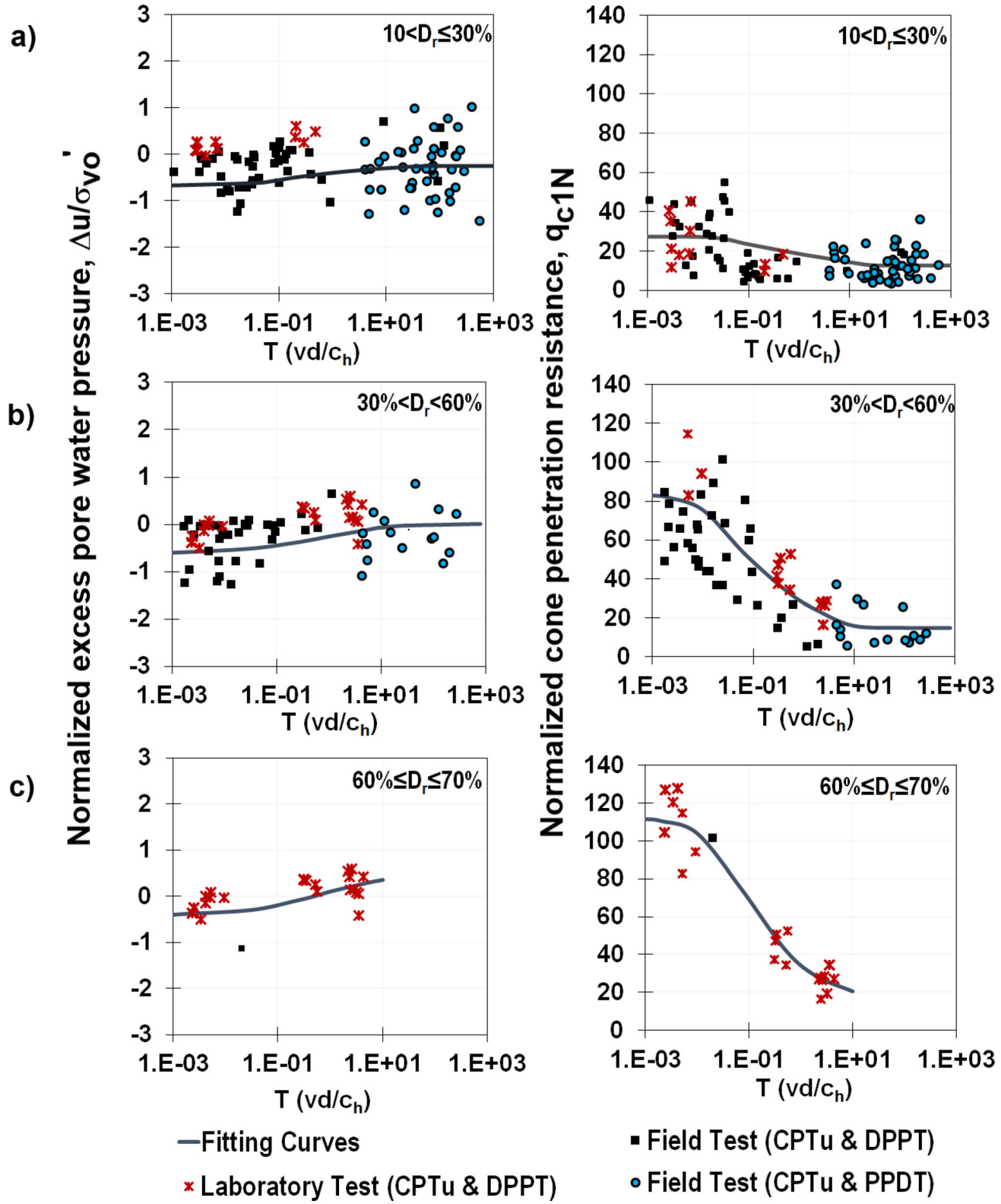

Fig. 12 Field and physical model test results from drained to undrained conditions: Effects of normalized penetration rate and relative density on excess pore water pressure, and cone penetration resistance at different relative density ranges of **a** $10 < D_r \leq 30\%$, **b** $30\% < D_r < 60\%$, and **c** $60\% \leq D_r \leq 70\%$

Table 2 Coefficients for a given relative density an drainage conditions

	Drainage condition	$10 \leq D_r < 30$		$30 \leq D_r \leq 60$		$60 < D_r \leq 70$	
		C_1	C_2	C_1	C_2	C_1	C_2
$\Delta u/\sigma_{vo}'$	Drain loading ($T < 1$)	0.005	− 0.579	0.009	− 0.535	0.032	− 0.186
	Partial drain loading ($0.01 < T < 10$)	0.036	− 0.447	0.075	− 0.255	0.104	0.091
	Undrain loading ($10 > T$)	0.001	− 0.275	0.016	− 0.061	n/a	n/a
q_{c1N}	Drain loading ($T < 1$)	− 0.869	23.000	− 2.129	64.53	− 2.274	94.827
	Partial drain loading ($0.01 < T < 10$)	− 2.009	17.358	− 8.547	30.79	− 12.580	41.624
	Undrain loading ($10 > T$)	− 0.156	13.468	− 0.324	16.45	n/a	n/a

5 Experimental test results with the field test data

The field and physical model test results were plotted together in Fig. 12a-c to understand the variation of $\Delta u/\sigma_{vo}$' and q_{c1N}, with a log-T for three distinct ranges of relative densities, from fully drained to undrained conditions. For ranges of D_r from 10 to 30% (loose soil), u/σ_{vo}' slightly increased and q_{c1N} slightly decreased, with an increase in T values (Fig. 12a). For D_r ranges from 30 to 60% (loose to medium dense soil) and from a T of 0.01 to 10, the u/σ_{vo}' increased and q_{c1N} decreased considerably (Fig. 12b). For ranges of D_r from 60 to 70% (dense soil), $\Delta u/\sigma_{vo}$' and q_{c1N} significantly changed, with an increase in T values between 0.01 to 10. As shown in Fig. 12c, at D_r ranges from 60 to 70%, only one data component was obtained from the field, and the rest of the data and trend was gained from the tests performed in the laboratory.

In general, for each relative density range above the T of 10, not much change was observed in $\Delta u/\sigma_{vo}$' and q_{c1N} with an increase in T. These results indicate that the $T_{undr,}$ which is the transition value of T from the partially drained to undrained response, is 10. The fines cause undrained conditions during penetration into the fine-grained soils. Ecemis [14] and Huang [18] also showed that low c_h (high T) is the main reason for lower effective stress at the cone tip in the sand with fines than in clean sand at the same D_r. Similarly, below a T of 0.01, the q_{c1N} and $\Delta u/\sigma_{vo}$' did not change with a decrease in T. These results indicate that T_{dr}, which is the transition value of T from the drained to partially drained response, is 0.01. These results imply that at different D_r values, the effect of T agrees perfectly well with the impact of penetration on the CPT resistance and excess pore pressure response.

Using the above field and laboratory test data, a logarithmic relationship was developed at drained, partially drained, and undrained conditions at different D_r ranges:

$$q_{c1N}, \frac{\Delta u}{\sigma'_{vo}} = C_1 \ln(T) + C_2 \tag{10}$$

where C_1 and C_2 are curve fitting coefficients that vary with the range of D_r and drainage conditions. The values of these coefficients are given in Table 2.

The limit T values found in this study for drained and undrained conditions during cone penetration were compared to other researchers [3, 8, 14, 18, 20, 21, 28, 30, 46]. Based on these researchers' findings, the drain and undrain boundary ranges were determined between 0.01 to 1, and 6 to 75, respectively. These limit ranges suggested by several researchers are reasonable when the results reported in this study are considered.

6 Conclusion

In this study, the sands and silty sands at different FCs (5%, 15%, and 35%) were prepared inside the rectangular large-scale soil box. Then, a group of twelve sets of tests (CPTu, SCPTu, and DPPT) were performed at different v, c_h, and D_r to understand the drainage conditions on u and q_{c1N}. The experimental test results have yielded the following significant findings:

In the first part of this study, the influences of D_r and FC on permeability, coefficient of consolidation, and compressibility were assessed to understand drainage conditions' effect on pore water pressure and cone penetration resistance during CPT tests. At the same density, the increase of FC over 5% significantly affects the pore size and permeability, and m_v is not greatly dependent on the FC of the soil. Hence, the change in c_h is directly related to the change in k. At different FCs, the difference of c_h is the most important reason for the different drainage conditions, which plays a vital role in the u development and q_{c1N}.

In the second part of this study, the influences of D_r and FC on the $\Delta u/\sigma_{vo}$' and q_{c1N} were assessed. Relative density and FC are shown to have a significant and complex effect on the $\Delta u/\sigma_{vo}$' values. The u is negative for dense soil, indicating soil dilation during the cone penetration process. At each FC, the $\Delta u/\sigma_{vo}$' reduces by an increase in D_r. Adding 5% silt to the sand increased its $\Delta u/\sigma_{vo}$' compared to the clean sand at a D_r less than 35%; however, the $\Delta u/\sigma_{vo}$' decreased as the soil became denser. The further addition of fines from 5 to 15% shifted trend lines of $\Delta u/\sigma_{vo}$' upward; however, at more than 15% FC, we examined an increase in $\Delta u/\sigma_{vo}$' for $D_r < 60\%$. As it is well known, for each FC, q_{c1N} increased with an increase in D_r. At a given D_r, the q_{c1N} decreased, with an increase in FC from 0 to 35%.

In the third part of this study, q_{c1N} and $\Delta u/\sigma_{vo}$' were examined over different T values with different relative densities. The T changed with a change in the cone penetration rate and the coefficient of consolidation. The laboratory test results show that positive $\Delta u/\sigma_{vo}$' developed at each T value for loose and medium-dense soils. For dense soils, as T gets smaller, an extensive amount of negative $\Delta u/\sigma_{vo}$' was measured. Compatibly, when T increased, q_{c1N} decreased for the soil at the same D_r. The reduction in q_{c1N} at dense and medium-dense soil is more evident than the reduction in loose soil.

In the fourth part of this study, the test results revealed from the laboratory were extended with the field test program performed by Ecemis and Karaman (2014). In the field tests, the T values changed only with a change in the c_h. The field test results clearly showed that c_h is very low in silty sand, and high excess pore pressure that occurs during penetration caused the dissipation time to take longer. This difference in sand and silty sand is the effect of drainage conditions.

The laboratory and field results revealed that T is a more consistent parameter than the fines to determine the q_c and u from the drainage conditions. In addition, T can be used to determine the drained, partially drained, and undrained responses during penetration of the cone into the soil. Under different D_r, the limits of T are quantified as follows: (1) the transition from partially drained to undrained penetration occurs around $T_{und} = 10$, since q_{c1N} and $_u/\sigma_{vo}$' almost stabilize at this value, and (2) the transition from partially drained to fully drained conditions occurs around $T_{dr} = 0.01$ due to a slight change in q_{c1N} when T is smaller than 0.01. Finally, a general equation is developed to determine the q_{c1N} and $\Delta u/\sigma_{vo}$' from the drainage conditions and relative density.

Author contributions All authors contributed to the study conception and design. Material preparation, data collection, and analysis were performed by All authors. All authors read and approved the final manuscript.

Funding The authors declare that no funds, grants, or other support were received during the preparation of this manuscript.

Data availability The datasets generated during and/or analyzed during the current study are not publicly available but are available from the corresponding author (Prof. Dr. Nurhan Ecemis) on reasonable request.

Declarations

Conflict of interest The authors have no relevant financial or non-financial interests to disclose.

References

1. Bandini P, Sathiskumar S (2009) Effects of silt content and void ratio on the saturated hydraulic conductivity and compressibility of sand-silt mixtures. J Geotech Geoenviron Eng 135(12):1976–1980. https://doi.org/10.1061/(asce)gt.1943-5606.0000177
2. Campanella RG, Stewart WP (1992) Seismic cone analysis using digital signal processing for dynamic site characterization. Can Geotech J 29(3):477–486. https://doi.org/10.1139/t92-052
3. Ceccato F, Simonini P (2017) Numerical study of partially drained penetration and pore pressure dissipation in piezocone test. Acta Geotech 12(1):195–209. https://doi.org/10.1007/s11440-016-0448-6
4. Chai J, Sheng D, Carter JP, Zhu H (2012) Coefficient of consolidation from non-standard piezocone dissipation curves. Comput Geotech 41:13–22. https://doi.org/10.1016/j.compgeo.2011.11.005
5. Chow SH, Bienen B, Randolph MF (2018) Rapid penetration of piezocones in sand. In: Proceedings of the 4th International Symposium on Cone Penetration Testing (CPT'18), Delft University of Technology, Netherlands. 213–219
6. Cubrinovski M (2019) Some important considerations in the engineering assessment of soil liquefaction. NZ Geomechanics News, Issue 97
7. Cubrinovski M, Rees S, Bowman E (2010) Chapter 6: effects of non-plastic fines on liquefaction resistance of sandy soils. In: Garevski M, Ansal A (eds) Earthquake engineering in Europe. Springer, pp 125–144
8. DeJong JT, Randolph MF (2012) Influence of partial consolidation during cone penetration on estimated soil behavior type and pore pressure dissipation measurements. J Geotech Geoenviron Eng. https://doi.org/10.1061/(ASCE)GT.1943-5606.0000646
9. Doan L, Lehane BM (2021) CPT data in normally consolidated soils. Acta Geotech 16(9):2877–2885
10. Duan W, Cai G, Liu S, Puppala AJ, Chen R (2019) In-situ evaluation of undrained shear strength from seismic piezocone penetration tests for soft marine clay in Jiangsu China. Transp Geotech. https://doi.org/10.1016/j.trgeo.2019.100253

11. Ecemis N (2013) Simulation of seismic liquefaction: 1-g model testing system and shaking table tests. Eur J Environ Civ Eng 17(10):899–919. https://doi.org/10.1080/19648189.2013.833140
12. Ecemis N, Karaman M (2014) Influence of non-/low plastic fines on cone penetration and liquefaction resistance. Eng Geol 181:48–57. https://doi.org/10.1016/j.enggeo.2014.08.012
13. Ecemis N (2014) Effects of permeability and compressibility on liquefaction assessment of silty soils using cone penetration resistance European Union Marie Curie Fellowship, FP7-PEOPLE-2009-RG, Proje No: PIRG05-GA-2009-248218
14. Ecemis N (2008) Effects of permeability and compressibility on liquefaction screening using cone penetration resistance. Ph.D. Thesis, Department of Civil Structural and Environmental Engineering, State University of New York at Buffalo, 282p
15. Ghali M, Chekired M, Karray M (2019) A laboratory-based study correlating cone penetration test resistance to the physical parameters of uncemented sand mixtures and granular soils. Eng Geol 255:11–25. https://doi.org/10.1016/j.enggeo.2019.04.015
16. Gui MW, Bolton MD, Garnier J, Corte JF, Bagge G. Laue J, Renzi, R (1998) Guidelines for cone penetration tests in sand. In: Int Conf Centrifuge 98, 155–160. A.A.Balkema, Brookfield: International Society for Soil Mechanics and Geotechnical Engineering (ISSMGE)
17. House AR, Oliveira JRMS, Randolph MF (2001) Evaluating the coefficient of consolidation using penetration tests. Int J Phy Model Geotech 1(3):17–25. https://doi.org/10.1680/ijpmg.2001.010302
18. Huang Q (2015) Effect of non-plastic fines on cone resistance in silty sands. Ph.D. Thesis, Department of Civil Structural and Environmental Engineering, State University of New York at Buffalo
19. Huang W, Sheng D, Sloan SW, Yu HS (2004) Finite element analysis of cone penetration in cohesionless soil. Comput Geotech 31(7):517–528. https://doi.org/10.1016/j.compgeo.2004.09.001
20. Jaeger RA, DeJong JT, Boulanger RW, Low HE, Randolph MF (2010) Variable penetration rate CPT in an intermediate soil. In: Proc., 2nd Int. Symp. on Cone Penetration Testing
21. Kim K, Prezzi M, Salgado R, Lee W (2008) Effect of penetration rate on cone penetration resistance in saturated clayey soils. J Geotech Geoenviron Eng 134(8):1142–1153
22. Krage CP, Broussard NS, DeJong JT (2014) Estimating rigidity index (I_R) based on CPT measurements. In: 3rd International Symposium on Cone Penetration Testing, Las Vegas, Nevada: 727–735
23. Kokusho T, Ito F, Nagao Y, Green AR (2012) Influence of non/low-plastic fines and associated aging effects on liquefaction resistance. J Geotech Geoenviron Eng 138(6):747–756. https://doi.org/10.1061/(asce)gt.1943-5606.0000632
24. Kumar J, Raju KVSB (2009) Miniature cone tip resistance of sand with fly ash using triaxial setup. Can Geotech J 46(2):231–240. https://doi.org/10.1139/T08-112
25. Lade PV, Liggio CDJ, Yamamuro JA (1998) Effects of non-plastic fines on minimum and maximum void ratios of sand. Geotech Test J 21(4):336–347
26. Lee DS, Elsworth D, Hryciw R (2008) Hydraulic conductivity measurement from on-the-fly uCPT sounding and from visCPT. J Geotech Geoenviron Eng 134(12):1720–1729. https://doi.org/10.1061/(asce)1090-0241(2008)134:12(1720)
27. Lo Presti D, Pallara O, Lancelotta R, Amandi M, Maniscalco R (1993) Monotonic and cyclic loading behavior of two sands at small strains. Geotech Test J 16(4):409–424
28. Mahmoodzadeh H, Randolph MF (2014) Penetrometer testing: Effect of partial consolidation on subsequent dissipation response. J Geotech Geoenviron Eng. https://doi.org/10.1061/(ASCE)GT.1943-5606.0001114
29. Mayne Paul W (2007) "Cone Penetration Testing." *NCHRP Synthesis of Highway Practice*.
30. Mlynarek Z, Gogolik S, Półtorak J (2012) The effect of varied stiffness of soil layers on interpretation of CPTU penetration characteristics. Archiv Civ Mech Eng 12:253–264. https://doi.org/10.1016/j.acme.2012.03.013
31. Oliveira JRMS, Almeida MSS, Motta HG, Almeida MCF (2011) Influence of penetration rate on penetrometer resistance. J Geotech Geoenviron Eng 137(7):695–703. https://doi.org/10.1061/(asce)gt.1943-5606.0000480
32. Olsen RS (1994) Normalization and Prediction of Geotechnical Properties using the Cone Penetrometer Test (CPT). Ph.D. Dissertation, University of California, Berkeley, CA
33. Parkin AK, Lunne T (1982) Boundary effects in the laboratory calibration of a cone penetration for sand. In: 2nd European Symposium on Penetration Testing, 1–7. Amsterdam: Norwegian Geotechnical Institute
34. Phillips R, Valsangkar AJ (1987) An experimental investigation of factors affecting penetration resistance in granular soils in centrifuge modelling. Technical Report, Department of Engineering, Cambridge University
35. Randolph MF, Hope S (2004) Effect of cone velocity on cone resistance and excess pore pressures. In: Proc. of the IS Osaka – Engineering Practice and Performance of Soft Deposits, edited by T. Matsui, Y. Tanaka, and M. Mimura, 147–152. Osaka: Yodogawa Kogisha Co. Ltd
36. Renzi R, Corte JF, Rault G, Bagge G (1994) Cone penetration tests in the centrifuge: Experience of five laboratories. In: Int. Conf. Centrifuge Testing 94, 77–82. A.A.Balkema, Rotterdam: International Society for Soil Mechanics and Foundation Engineering (ISSMFE)
37. Robertson PK, Campanella RG, Gillespie D, Greig J (1986) Use of piezometer cone data. In: Proc., In-Situ 86 Specialty Conference, 1263–1280. Blacksburg: American Society of Civil Engineers
38. Schneider JA, Lehane BM, Schnaid F (2007) Velocity effects on piezocone tests in normally and overconsolidated clays. Int J Phy Model Geotech 7(2):23–34. https://doi.org/10.1680/ijpmg.2007.070202
39. Senders M (2010) Cone resistance profiles for laboratory tests in sand. In: Proceedings of the 2nd International Conference on Cone Penetration Testing, Huntington Beach, Calif. 2010; Paper No. 2–08.
40. Sully JP, Robertson PK, Campanella RG, Woeller DJ (1999) An approach to evaluation of field CPTu dissipation data in over consolidated fine-grained soils. Can Geotech J 36(2):369–381. https://doi.org/10.1139/t98-105
41. Susila E, Hryciw RD (2003) Large displacement FEM modelling of the cone penetration test (CPT) in normally consolidated sand. Int J Num Analy Meth Geomech 27(7):585–602. https://doi.org/10.1002/nag.287
42. Suwal LP, Kuwano R (2012) Poisson's ratio evaluation on silty and clayey sands on laboratory specimens by flat disk shaped piezo-ceramic transducer. Bulletin of ERS: 45
43. Teh CI, Houlsby GT (1991) An analytical study of the cone penetration test in clay. Geotechnique 41(1):17–34. https://doi.org/10.1680/geot.1991.41.1.17
44. Thevanayagam S, Ecemis N (2008) Effects of permeability on liquefaction resistance and cone resistance. Geotech Spe Pub 181:1–11. https://doi.org/10.1061/40975(318)92
45. Yamamuro JA, Convert KM (2001) Monotonic and cyclic liquefaction of very loose sands with high silt content. J Geotech Geoenviron Eng ASCE 127(4):314–324. https://doi.org/10.1061/(ASCE)1090-0241(2001)127:4(314)
46. Yamamuro JA, Wood FM (2004) Effect of depositional method on the undrained behavior and microstructure of sand with silt.

Soil Dyn Earth Eng 24(9–10):751–760. https://doi.org/10.1016/j.soildyn.2004.06.004
47. Yi JT, Goh SH, Lee FH, Randolph MF (2012) A numerical study of cone penetration in fine grained soils allowing for consolidation effects. Geotechnique 62(8):707–719. https://doi.org/10.1680/geot.8.P.155
48. Zhao Z, Congress SSC, Cai G, Duan W (2022) Bayesian probabilistic characterization of consolidation behavior of clays using CPTU data. Acta Geotech 17:931–948. https://doi.org/10.1007/s11440-021-01277-8